Fully-automated identification of fish species based on otolith contour: using short-time Fourier transform and discriminant analysis (STFT-DA)

Nima Salimi, Kar Hoe Loh, Sarinder Kaur Dhillon, Ving Ching Chong

Background. Fish species may be identified based on their unique otolith shape or contour. Several pattern recognition methods have been proposed to classify fish species through morphological features of the otolith contours. However, there has been no fully-automated species identification model with the accuracy higher than 80%. The purpose of the current study is to develop a fully-automated model, based on the otolith contours, to identify the fish species with the high classification accuracy. Methods. Images of the right sagittal otoliths of 14 fish species from three families namely Sciaenidae, Ariidae, and Engraulidae were used to develop the proposed identification model. Short-time Fourier transform (STFT) was used, for the first time in the area of otolith shape analysis, to extract important features of the otolith contours. Discriminant Analysis (DA), as a classification technique, was used to train and test the model based on the extracted features. Results. Performance of the model was demonstrated using species from three families separately, as well as all species combined. Overall classification accuracy of the model was greater than 90% for all cases. In addition, effects of STFT variables on the performance of the identification model were explored in this study. Conclusions. Short-time Fourier transform could determine important features of the otolith outlines. The fully-automated model proposed in this study (STFT-DA) could predict species of an unknown specimen with acceptable identification accuracy. The current model has flexibility to be used for more species and families in future studies.

PeerJ PrePrints | https://dx.doi.org/10.7287/peerj.preprints.1517v1 | CC-BY 4.0 Open Access | rec: 19 Nov 2015, publ: 19 Nov 2015

Fully-automated identification of fish species based on otolith contour: using short-time Fourier transform and discriminant analysis (STFT-DA)

Nima Salimi [1], Kar Hoe Loh [2], Sarinder Kaur Dhillon [1], Ving Ching Chong [1,2]

[1] Institute of Biological Sciences, University of Malaya, Kuala Lumpur, Federal Territory KL, 50603, Malaysia

[2] Institute of Ocean & Earth Sciences, University of Malaya, Kuala Lumpur, Federal Territory KL, 50603, Malaysia

Corresponding Author:

Ving Ching Chong [1,2]

Institute of Biological Sciences, University of Malaya, Kuala Lumpur, Federal Territory KL, 50603, Malaysia

Email address: chong@um.edu.my

PeerJ PrePrints | https://dx.doi.org/10.7287/peerj.preprints.1517v1 | CC-BY 4.0 Open Access | rec: 19 Nov 2015, publ: 19 Nov 2015

Abstract

Background. Fish species may be identified based on their unique otolith shape or contour. Several pattern recognition methods have been proposed to classify fish species through morphological features of the otolith contours. However, there has been no fully-automated species identification model with the accuracy higher than 80%. The purpose of the current study is to develop a fully-automated model, based on the otolith contours, to identify the fish species with the high classification accuracy.

Methods. Images of the right sagittal otoliths of 14 fish species from three families namely Sciaenidae, Ariidae, and Engraulidae were used to develop the proposed identification model. Short-time Fourier transform (STFT) was used, for the first time in the area of otolith shape analysis, to extract important features of the otolith contours. Discriminant Analysis (DA), as a classification technique, was used to train and test the model based on the extracted features.

Results. Performance of the model was demonstrated using species from three families separately, as well as all species combined. Overall classification accuracy of the model was greater than 90% for all cases. In addition, effects of STFT variables on the performance of the identification model were explored in this study.

Conclusions. Short-time Fourier transform could determine important features of the otolith outlines. The fully-automated model proposed in this study (STFT-DA) could predict species of an unknown specimen with acceptable identification accuracy. The current model has flexibility to be used for more species and families in future studies.

INTRODUCTION

Automated taxon identification (ATI) systems which rely on pattern recognition and machine learning techniques have been developed in different areas of biology (Arbuckle et al. 2001; Chun et al. 2007; Cope et al. 2012; Culverhouse et al. 1996; Dietrich & Pooley 1994; Farr & Chesmore 2007; Gaston & O'Neill 2004; Jonker et al. 2000; La Salle et al. 2009; Larios et al. 2008; MacLeod et al. 2010; Parisi-Baradad et al. 2010; Potamitis 2014; Watson et al. 2003; Watson & Dallwitz 1991; Zhao et al. 2013). In marine biology, identification of the fish species based on the otolith image analysis has been an interesting area due to its applications in the palaeontological and ecological sciences (Aguirre & Lombarte 1999; Arellano et al. 1995; Bowen 2000; Fitch & Brownell Jr 1968; Lombarte & Castellón 1991; Reichenbacher et al. 2007). Parisi et al. (2010) developed the first automated taxon classification system through the shape analysis of the otolith contour. In order to extract the important morphological features of the otolith contour, external outline of the otolith was first converted to a one-dimensional (1D) signal. This representative signal was obtained by calculating the distances between the outline points and the center of gravity of the otolith image. Then, wavelet transform (WT) was applied on the 1D signal to extract useful features of the otolith outline. Using WT, irregularities of the otolith contours were quantified and localized appropriately; this is the advantage of WT over other feature extractors such as Fourier transform (FT) and elliptical Fourier descriptors (EFD) used in the other studies (Parisi-Baradad et al. 2005; Sadighzadeh et al. 2012). Even though their proposed model could identify the family of the specimens with 94% accuracy, the performance of the system dropped significantly at the species level (72%) (Parisi-Baradad et al. 2010). Therefore, the aim of the present study is to develop a fully-automated identification model with improved classification accuracy at the level of species. Fourteen fish species from three different families namely Engraulidae, Sciaenidae, and Ariidae were used in this study. Short-time Fourier transform (STFT) is a conventional signal processing technique (Allen 1997; Buck et al. 1999; Rabiner & Schafer 1978) which to our knowledge has not yet been employed in the area of otolith image processing. STFT was applied in this study to extract morphological features of the otolith contours.

PeerJ PrePrints | https://dx.doi.org/10.7287/peerj.preprints.1517v1 | CC-BY 4.0 Open Access | rec: 19 Nov 2015, publ: 19 Nov 2015

MATERIALS AND METHODS

Images of the right sagittal otoliths were captured using a stereomicroscope (Olympus DP25FW, 6.3X magnification) attached with a digital camera. Proximal view of the otolith, dorsal edge facing up and posterior end facing the positive direction, was used in this study. The proposed image identification system was implemented in MATLAB (MATLAB® Release 2013a, The MathWorks, Inc., Kuala Lumpur, Malaysia). Figure 1 illustrates the schematic diagram of the fully-automated image recognition model represented in this study. Different stages of this system are detailed as follows.

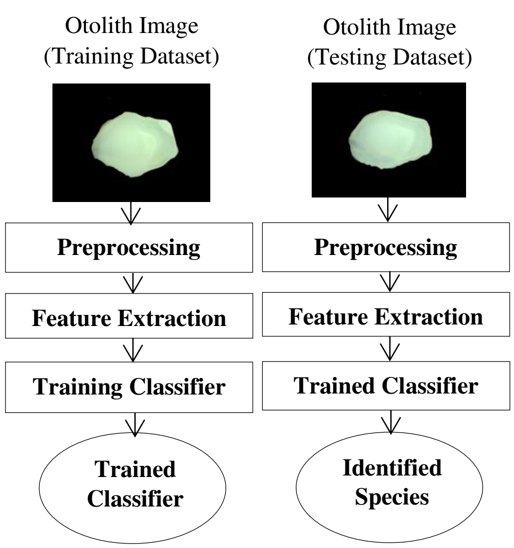

Figure 1 A schematic diagram of the proposed image identification system. The left panel shows different stages for training the model, and the testing part of the system is illustrated in the right panel.

Preprocessing

Discrimination among different fish species was based on the 1D representation of the otolith outline. Firstly, the external outline of the surface contours of the otolith had to be extracted and then, distances between the center of gravity and the contour points had to be calculated. For this

PeerJ PrePrints | https://dx.doi.org/10.7287/peerj.preprints.1517v1 | CC-BY 4.0 Open Access | rec: 19 Nov 2015, publ: 19 Nov 2015

purpose, the grayscale image of the otolith was converted to the binary image with the threshold value of 0.1. Choice of this threshold value (0.1) resulted in obtaining the binary images for the otoliths with a wide range of transparency. After clearing the borders and filling the holes, the small objects (objects that had fewer than 50000 pixels) were removed from the binary images. Then, coordinates of the boundary (outline) pixels as well as the center of gravity were calculated. By having these coordinates, characteristic 1D signals, which are the distances between the boundary pixels and center of gravity as a function of the corresponding angles, were determined. Figure 2 shows an image of the otolith with its representative 1D signal.

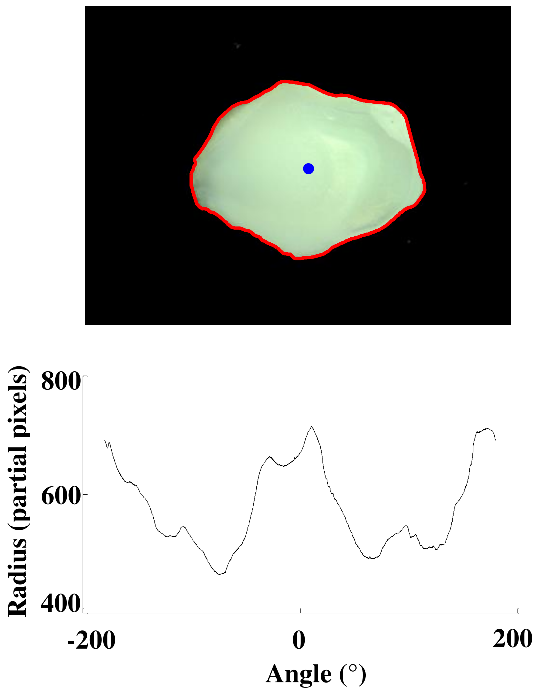

Figure 2 Image of an otolith (upper panel) with its corresponding 1D signal (lower panel). 1D signal was obtained by calculating the radius, distances between the boundary pixels (red) and the center of gravity (blue), as a function of angle.

Feature Extraction

1D signals obtained from the previous stage were down-sampled to 1000 points (samples) by interpolation using fast Fourier transform (FFT). In this study, short-time Fourier transform (STFT) was applied as a feature extraction method on the resampled signals. STFT of the original (1D) signals were determined by using 100-point Gaussian window with 40 overlapped samples (totally 16 segments for each signal). Type of the windowing function affected the performance of the identification system. To explore this effect, results obtained using different windowing techniques were compared in the next section. Figure 3 shows the spectrogram (using STFT) obtained from 1D signal illustrated in fig. 2. Each segment of the original signal consisted of 129 frequency components. Absolute values and phase angles of the frequency components of each segment were determined and then standardized by calculating the corresponding z-scores (Z_ABSs: z-scores of the absolute values and Z_ANGs: z-scores of the angles). In each segment of the signal, two important parameters were determined: maximum of the Z_ABSs (MAX_{ABS}) and maximum of Z_ANGs (MAX_{ANG}). Having 16 segments in each signal, 32 attributes (16 MAX_{ABS} + 16 MAX_{ANG}) were extracted from each representative signal. By this way, each otolith image could be converted to a 32- element vector in which the first 16 elements were MAX_{ABS} values and the rest were the values of MAX_{ANG}.

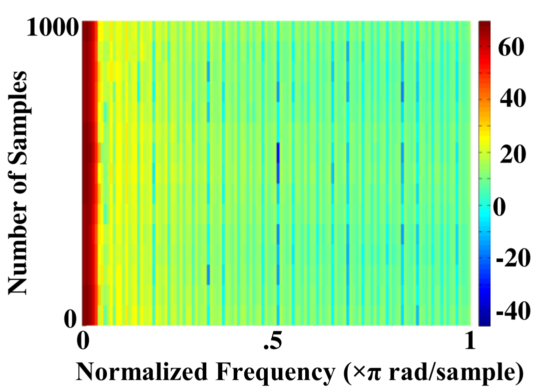

Figure 3 The spectrogram of the characteristic signal shown in fig. 2. The original signal was resampled to 1000 points before calculating the short-time Fourier transform (STFT).

Classification

The characteristic vectors obtained from the previous stage were utilized as inputs to the Discriminant Analysis (DA) classifier in order to train and test the identification system. Fourteen species from three different families were used in this study (Table 1). All otoliths were extracted from fish obtained from fish landing sites or the wet markets. No ethics clearance was required from the University of Malaya – Institutional Animal Care and Use Committee (UM-IACUC).

Table 1. Fish species used in the proposed fully-automated identification system.

Species	Family
Dendrophysa russelli	Sciaenidae
Johnius belangerii	″
Johnius carouna	″
Otolithes ruber	″
Panna microdon	″
Nemapteryx caelata	Ariidae
Arius maculatus	″
Cryptarius truncatus	″
Hexanematichtys sagor	″
Osteogeneiosus militaris	″
Plicofollis argyropleuron	″
Coilia dussumieri	Engraulidae
Setipinna taty	″
Thryssa hamiltonii	″

RESULTS

Three different fish families (Sciaenidae, Ariidae, and Engraulidae) were used separately to train and test the model. In addition, the proposed image identification model was evaluated for all 14 species combined.

Engraulidae Family

Three species namely *Coilia dussumieri*, *Setipinna taty* and *Thryssa hamiltonii* from the Engraulidae family were used in this study. From each species, 20 specimens (otolith images) were used for training the model. Then, the trained model was tested with 10 specimens per species (total of 30 images for testing the model). Table 2 demonstrates the confusion matrix obtained from the predicted species in this family.

Table 2. Confusion matrix for the classification results of the Engraulidae family. The predicted species (columns) are compared with the species confirmed by an expert (rows).

	Coilia dussumieri	*Setipinna taty*	*Thryssa hamiltonii*
Coilia dussumieri	**10 (100%)**	0 (0%)	0 (0%)
Setipinna taty	0 (0%)	**10 (100%)**	0 (0%)
Thryssa hamiltonii	0 (0%)	1 (10%)	**9 (90%)**

All of the 10 specimens from the *Coilia sussumieri* and *Setipinna taty* species were classified correctly. For the *Thryssa hamiltonii* species, one specimen was misclassified as the *Setipinna taty* species. In the overall, 29 out of 30 specimens from the Engraulidae family (~ 97%) were correctly predicted as the target species.

Sciaenidae Family

Five species of the Sciaenidae family were also used to evaluate performance of the identification system. In this family, 19 specimens per species (total number of 95 specimens) were used to train the system, and then the trained model was tested with 50 specimens (10 specimens per species). The predicted results of this family are presented in Table 3. Among five species in this family, three species (*Johnius belangerii*, *Johnius carouna*, and *Panna microdon*) were identified with 100% accuracy. Two other species (*Dendrophysa russelli* and *Otolithes ruber*) had one misclassified specimen each. In this family, similar to the Engraulidae family, there was no species with a classification accuracy of less than 90%. The proposed model could identify five species of the Sciaenidae family with an overall accuracy of 96%.

Table 3. Confusion matrix obtained from five species of the Sciaenidae family. The columns indicate the predicted species by the identification model, while rows indicate the target species.

	Dendrophysa russelli	*Johnius belangerii*	*Johnius carouna*	*Otolithes ruber*	*Panna microdon*
Dendrophysa russelli	**9 (90%)**	0 (0%)	0 (0%)	1 (10%)	0 (0%)
Johnius belangerii	0 (0%)	**10 (100%)**	0 (0%)	0 (0%)	0 (0%)
Johnius carouna	0 (0%)	0 (0%)	**10 (100%)**	0 (0%)	0 (0%)
Otolithes ruber	1 (10%)	0 (0%)	0 (0%)	**9 (90%)**	0 (0%)
Panna microdon	0 (0%)	0 (0%)	0 (0%)	0 (0%)	**10 (100%)**

Ariidae Family

Six species from the Ariidae family were also used in this study. The number of specimens per species for training and testing the model were 18 and 10, respectively. The classification results obtained from this family are shown in table 4. Overall accuracy of the model in this family was ~93% which is slightly less than the other two families. The lowest classification accuracy (80%) in this family was for the *Nemapteryx caelatus.* Two specimens of the *Nemapteryx caelatus* *species* were predicted as the *Cryptarius truncatus.* Three species namely *Arius maculatus*, *Hexanematichtys sagor* and *Plicofollis argyropleuron* had 100% correct prediction results. The accuracy of the model for the *Cryptarius truncatus* and *Osteogeneiosus militaris* species was 90%. Both of these species had one specimen that was misclassified as *Nemapteryx caelatus*.

Table 4. Classification results (confusion matrix) of the Ariidae family. Outputs of the identification model (columns) are compared with the target species (rows).

	Nemapteryx caelatus	*Arius maculatus*	*Cryptarius truncatus*	*Hexanematichtys sagor*	*Osteogeneiosus militaris*	*Plicofollis argyropleuron*
Nemapteryx caelatus	**8 (80%)**	0 (0%)	2 (20%)	0 (0%)	0 (0%)	0 (0%)
Arius maculatus	0 (0%)	**10 (100%)**	0 (0%)	0 (0%)	0 (0%)	0 (0%)
Cryptarius truncatus	1 (10%)	0 (0%)	**9 (90%)**	0 (0%)	0 (0%)	0 (0%)
Hexanematichtys sagor	0 (0%)	0 (0%)	0 (0%)	**10 (100%)**	0 (0%)	0 (0%)
Osteogeneiosus militaris	1 (10%)	0 (0%)	0 (0%)	0 (0%)	**9 (90%)**	0 (0%)
Plicofollis argyropleuron	0 (0%)	0 (0%)	0 (0%)	0 (0%)	0 (0%)	**10 (100%)**

All Three Families

To test the model with more species, all three families were combined (total number of 14 species) and the results of the classification are demonstrated in Table 5. From each species, 18 and 10 specimens were used to train and test the model, respectively (total numbers of 252 images for the training and 140 images for the testing). All 14 species were predicted by the proposed model with an overall accuracy of ~92%. Eight of these species, three from the Sciaenidae, three from the Ariidae, and two from the Engraulidae family, were classified with the accuracy of 100%. Three species showed the identification accuracy of less than 90% (*Dendrophysa russelli*: 80%, *Nemapteryx caelatus*: 70%, and *Cryptarius truncatus*: 70%). Both *Nemapteryx caelatus* and *Cryptarius truncatus* from the Ariidae family had the most numbers of misclassified specimens among the 14 species used in this study. The classification accuracy for *Otolithes ruber, Osteogeneiosus militaris,* and *Setipinna taty* was 90%. It is worth-noting that there was no cross-family misclassification for all six species that had at least one misclassified specimen (all six species had specimens correctly classified in their families). As a result, developing a model that first identifies the family and then species cannot lead to an improvement in the overall accuracy of the system.

Table 5. Confusion matrix for the identification results obtained from 14 species of three different families. In each target species (rows), numbers of specimens are indicated in the corresponding predicted species (columns). Species are *Dendrophysa russelli* (1), *Johnius belangerii* (2), *Johnius carouna* (3), *Otolithes ruber* (4), *Panna microdon* (5), *Nemapteryx caelatus* (6), *Arius maculatus* (7), *Cryptarius truncatus* (8), *Hexanematichtys sagor* (9), *Osteogeneiosus militaris* (10), *Plicofollis argyropleuron* (11), *Coilia dussumieri* (12), *Setipinna taty* (13), *Thryssa hamiltonii* (14).

	1	2	3	4	5	6	7	8	9	10	11	12	13	14
1	**8**	0	0	2	0	0	0	0	0	0	0	0	0	0
2	0	**10**	0	0	0	0	0	0	0	0	0	0	0	0
3	0	0	**10**	0	0	0	0	0	0	0	0	0	0	0
4	1	0	0	**9**	0	0	0	0	0	0	0	0	0	0
5	0	0	0	0	**10**	0	0	0	0	0	0	0	0	0
6	0	0	0	0	0	**7**	0	2	0	0	1	0	0	0
7	0	0	0	0	0	0	**10**	0	0	0	0	0	0	0

8	0	0	0	0	0	3	0	**7**	0	0	0	0	0	0
9	0	0	0	0	0	0	0	0	**10**	0	0	0	0	0
10	0	0	0	0	0	0	0	1	0	**9**	0	0	0	0
11	0	0	0	0	0	0	0	0	0	0	**10**	0	0	0
12	0	0	0	0	0	0	0	0	0	0	0	**10**	0	0
13	0	0	0	0	0	0	0	0	0	0	0	0	**9**	1
14	0	0	0	0	0	0	0	0	0	0	0	0	0	**10**

Effect of the windowing function

As mentioned in section 2, the windowing function used to calculate STFT of the representative signals could influence the performance of the model. To explore this effect, the identification system was trained and tested with several types of the window function. The overall accuracy obtained from three families, as well as the combined families, are compared and shown in Table 6.

Table 6. Classification results of the model for 16 different window functions. Using each window function (rows), the model performance was calculated for all four datasets (columns).

Window Functions	**Overall Accuracy**			
	Engraulidae Family	**Sciaenidae Family**	**Ariidae Family**	**All Families**
Bartlett-Hann	87%	82%	85%	83%
Bartlett	90%	82%	90%	85%
Blackman	60%	80%	88%	77%
Blackman-Harris	50%	80%	85%	62%
Bohman	53%	82%	87%	63%

Chebyshev	47%	78%	78%	69%
Flat Top	40%	68%	80%	64%
Gaussian	**97%**	**96%**	**93%**	92%
Hamming	93%	**96%**	92%	92%
Hann	70%	88%	88%	84%
Kaiser	90%	**96%**	82%	93%
Nuttall's	57%	84%	85%	68%
Parzen	50%	68%	90%	66%
Rectangular	87%	**96%**	83%	**94%**
Tapered cosine	93%	88%	87%	89%
Triangular	57%	84%	90%	84%

Using the Gaussian window function led to the highest classification accuracy (97%) in the Engraulidae family. In the Sciaenidae family, the best result (96%) was achieved by using four functions namely Gaussian, Hamming, Kaiser, and Rectangular. The most accurate prediction (93%) in the Ariidae family was obtained by using the Gaussian function. In the combined families, using the Rectangular function resulted in the highest overall accuracy (94%). However, utilizing the Rectangular windowing function led to relatively poor performance of the model in the Engraulidae (87%) and Ariidae (83%) families. Taking into accounts all the results obtained using these 16 functions, the Gaussian window function was selected in this study due to its good performance in all the four data sets.

PeerJ PrePrints | https://dx.doi.org/10.7287/peerj.preprints.1517v1 | CC-BY 4.0 Open Access | rec: 19 Nov 2015, publ: 19 Nov 2015

Discussion

The identification model proposed in this study could predict the species of an unknown specimen from the Engraulidae, Sciaenidae**,** and Ariidae family with the overall accuracy of 97%, 96%, and 93%, respectively. Even after combining three families the accuracy of the model remained above 90% (~ 92%), which is noticeably higher than the results obtained by the identification model proposed in the most related study (~ 72%) (Parisi-Baradad et al. 2010). It is noted that training data sets used in the present study were relatively small (19, 20, and 18 specimens per species for Sciaenidae, Engraulidae, and Ariidae family, respectively). Using more samples in the training sets could lead to increasing the accuracy of the model.

Two spectral analysis methods namely Fourier transform (FT) and wavelet transform (WT) have been applied in the previous studies as the feature extractors (Castonguay et al. 1991; Parisi-Baradad et al. 2005; Parisi-Baradad et al. 2010). Short-time Fourier transform (STFT) has been utilized in the present study, for the first time in the area of otolith image recognition, to analyse the spectrum of the 1D signal obtained from the fish otolith contour. As was demonstrated in section 3 (Table 6), the choice of window function had a direct effect on the performance of the system. In addition to the type of windowing function, the number of points of the window function and the number of overlapped samples played important roles in the classification results. The proposed model was also tested with a variety of these two parameters (not reported here), and the best match was selected (100-points Gaussian function with 40 overlapped samples).

In this study, only proximal view of the otolith image was used to develop the identification model. However, adding other views (e.g. anterior, dorsal) could lead to improving the performance of the model. Adding other views would be more crucial when other families and species are added to the system. The same procedure explained in section 2 can be applied on the other views of the otolith image. The other types of the window function could be more effective in analyzing the other views. In that case, a 32-element vector (section 2.2) can be extracted from each view of the otolith. Consequently, each specimen can be represented by a combination of up to six vectors (depending on the number of views), rather than only one vector corresponding to the proximal view. By this way, more important morphological features could be extracted from the otolith contours.

Two classification techniques namely Decision Tree and Discriminant Analysis were tested in this study (the results obtained by the Decision Tree are not shown here) and the latter was selected due to more accurate results. However, there are other classification methods such as Naive Bayes, Nearest Neighbors, Support Vector Machine, and Neural Network which may improve the performance of the model in the future studies.

Conclusions

A fully-automated identification system (STFT-DA) has been proposed in this study to classify the fish species based on the morphological characteristics of the otolith outline contour. Fourteen species from three families were used to develop and evaluate performance of the model. Combining the short-time Fourier transform (STFT), as the feature extractor, with the Discriminant Analysis (DA), as the classifier, led to improving the accuracy of the species classification in comparison with the existing automated model. The STFT window function as

PeerJ PrePrints | https://dx.doi.org/10.7287/peerj.preprints.1517v1 | CC-BY 4.0 Open Access | rec: 19 Nov 2015, publ: 19 Nov 2015

well as classification technique had significant effects on the performance of the model. Future enhancements of the proposed model may be needed to include more species into the system.

FUNDING

This work was supported by University of Malaya Research Grants (UMRG), RP008-2012C and RP008-2012A.

Acknowledgements

We would like to thank Cecilia Chu and Suellina Binti Sulaiman for capturing the otolith images. The University of Malaya is acknowledged for providing research facilities.

REFERENCES

Aguirre H, and Lombarte A. 1999. Ecomorphological comparisons of sagittae in Mullus barbatus and M. surmuletus. *Journal of Fish Biology* 55:105-114.

Allen J. 1997. Short term spectral analysis, synthesis, and modification by discrete Fourier transform. IEEE Trans on Acoust, Speech, and Sig Proc. p 21-24.

Arbuckle T, Schröder S, Steinhage V, and Wittmann D. 2001. Biodiversity informatics in action: identification and monitoring of bee species using ABIS. Proc 15th Int Symp Informatics for Environmental Protection. p 425-430.

Arellano R, Hamerlynck O, Vincx M, Mees J, Hostens K, and Gijselinck W. 1995. Changes in the ratio of the sulcus acusticus area to the sagitta area of Pomatoschistus minutus and P. lozanoi (Pisces, Gobiidae). *Marine Biology* 122:355-360.

Bowen W. 2000. Reconstruction of pinniped diets: accounting for complete digestion of otoliths and cephalopod beaks. *Canadian Journal of Fisheries and Aquatic Sciences* 57:898-905.

Buck JR, Oppenheim AV, and Schafer RW. 1999. Discrete-time signal processing. *ed Prentice Hall*.

Castonguay M, Simard P, and Gagnon P. 1991. Usefulness of Fourier analysis of otolith shape for Atlantic mackerel (Scomber scombrus) stock discrimination. *Canadian Journal of Fisheries and Aquatic Sciences* 48:296-302.

Chun J, Lee J-H, Jung Y, Kim M, Kim S, Kim BK, and Lim Y-W. 2007. EzTaxon: a web-based tool for the identification of prokaryotes based on 16S ribosomal RNA gene sequences. *International Journal of Systematic and Evolutionary Microbiology* 57:2259-2261.

Cope JS, Corney D, Clark JY, Remagnino P, and Wilkin P. 2012. Plant species identification using digital morphometrics: A review. *Expert Systems with Applications* 39:7562-7573.

Culverhouse PF, Simpson R, Ellis R, Lindley J, Williams R, Parsini T, Reguera B, Bravo I, Zoppoli R, and Earnshaw G. 1996. Automatic classification of field-collected dinoflagellates by artificial neural network. *Marine Ecology Progress Series* 139:281-287.

Dietrich CH, and Pooley CD. 1994. Automated identification of leafhoppers (Homoptera: Cicadellidae: Draeculacephala Ball). *Annals of the Entomological Society of America* 87:412-423.

Farr I, and Chesmore D. 2007. Automated bioacoustic detection and identification of wood-boring insects for quarantine screening and insect ecology. Proceedings of the International Conference on Bioacoustics. p 201-208.

Fitch JE, and Brownell Jr RL. 1968. Fish otoliths in cetacean stomachs and their importance in interpreting feeding habits. *Journal of the Fisheries Board of Canada* 25:2561-2574.

Gaston KJ, and O'Neill MA. 2004. Automated species identification: why not? *Philosophical Transactions of the Royal Society of London B: Biological Sciences* 359:655-667.

Jonker R, Groben R, Tarran G, Medlin L, Wilkins M, García L, Zabala L, and Boddy L. 2000. Automated identification and characterisation of microbial populations using flow cytometry: the AIMS project. *Scientia Marina* 64:225-234.

La Salle J, Wheeler Q, Jackway P, Winterton S, Hobern D, and Lovell D. 2009. Accelerating taxonomic discovery through automated character extraction. *Zootaxa* 2217:43-55.

Larios N, Deng H, Zhang W, Sarpola M, Yuen J, Paasch R, Moldenke A, Lytle DA, Correa SR, and Mortensen EN. 2008. Automated insect identification through concatenated histograms of local appearance features: feature vector generation and region detection for deformable objects. *Machine Vision and Applications* 19:105-123.

Lombarte A, and Castellón A. 1991. Interspecific and intraspecific otolith variability in the genus Merluccius as determined by image analysis. *Canadian journal of zoology* 69:2442-2449.

MacLeod N, Benfield M, and Culverhouse P. 2010. Time to automate identification. *Nature* 467:154-155.

Parisi-Baradad V, Lombarte A, García-Ladona E, Cabestany J, Piera J, and Chic O. 2005. Otolith shape contour analysis using affine transformation invariant wavelet transforms and curvature scale space representation. *Marine and Freshwater Research* 56:795-804.

Parisi-Baradad V, Manjabacas A, Lombarte A, Olivella R, Chic Ò, Piera J, and García-Ladona E. 2010. Automated Taxon Identification of Teleost fishes using an otolith online database—AFORO. *Fisheries Research* 105:13-20.

Potamitis I. 2014. Automatic classification of a taxon-rich community recorded in the wild.

Rabiner LR, and Schafer RW. 1978. *Digital processing of speech signals*: Prentice Hall.

Reichenbacher B, Sienknecht U, Küchenhoff H, and Fenske N. 2007. Combined otolith morphology and morphometry for assessing taxonomy and diversity in fossil and extant killifish (Aphanius,† Prolebias). *Journal of Morphology* 268:898-915.

Sadighzadeh Z, Tuset VM, Valinassab T, Dadpour MR, and Lombarte A. 2012. Comparison of different otolith shape descriptors and morphometrics for the identification of closely related species of Lutjanus spp. from the Persian Gulf. *Marine Biology Research* 8:802-814.

Watson AT, O'Neill MA, and Kitching IJ. 2003. Automated identification of live moths (Macrolepidoptera) using digital automated identification system (daisy). *Systematics and Biodiversity* 1:287-300.

Watson L, and Dallwitz MJ. 1991. The families of angiosperms: automated descriptions, with interactive identification and information retrieval. *Australian Systematic Botany* 4:681-695.

Zhao G, Krishnamurthy S, Cai Z, Popov VL, Travassos da Rosa AP, Guzman H, Cao S, Virgin HW, Tesh RB, and Wang D. 2013. Identification of novel viruses using VirusHunter–an automated data analysis pipeline. *PLoS One* 8:e78470.